ACS Macro Letters

Letter

pubs.acs.org/macroletters

Thin Films Constructed by Centrifugal Deposition of Highly Deformable, Charged Microgels

Xiaobo Hu[†] and L. Andrew Lyon*[,‡]

[†]School of Chemistry & Biochemistry, Georgia Institute of Technology, Atlanta, Georgia 30332, United States

[‡]Schmid College of Science and Technology, Chapman University, Orange, California 92866, United States

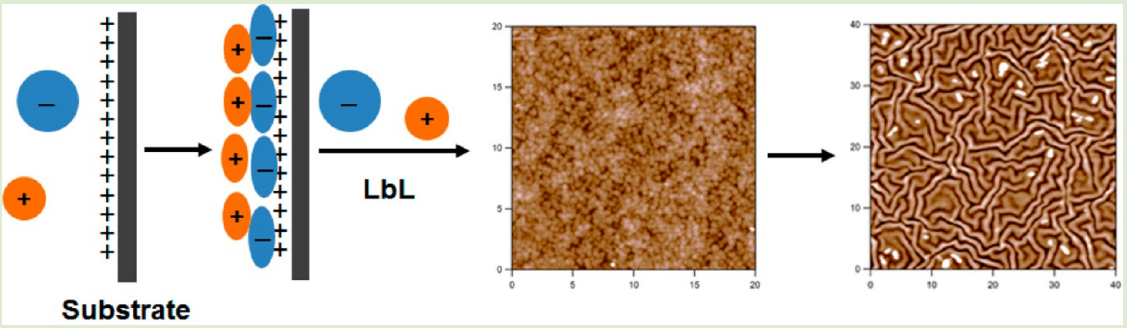

ABSTRACT: Thin films composed entirely of microgel building blocks were fabricated using two kinds of self-cross-linked, oppositely charged microgels, via centrifugal deposition. Atomic force microscopy studies revealed that both microgels form very thin monolayer films due to a large degree of microgel deformation during deposition. Meanwhile, centrifugal deposition from a mixture of these two kinds of microgels resulted in the formation of microgel bilayers with a total thickness of around 20 nm. The film thickness increased linearly with the deposition time. Additionally, isotropic stretching/release by heating/cooling of the dried microgel films generated complicated buckling patterns, while anisotropic (uniaxial) stretching/release resulted in parallel buckling perpendicular to the stretching direction. The damage caused by anisotropic stretching and 100 °C treatment can be healed by addition of water, while damage caused via treatment at 150 °C cannot be healed due to the occurrence of polymer cross-linking, which inhibits the mobility of the microgel building blocks.

During the past few decades, the fabrication of films by layer-by-layer (LbL) assembly technology has attracted great interest. Various components, such as synthetic polymers, biomacromolecules, dendritic molecules, polymeric microgels, colloidal particles, or complexes of these species, can be used as building blocks to form films with a thickness ranging from nanometers to micrometers on different substrates.[1−8] Since our first paper on microgel films using poly(*N*-isopropylacrylamide-acrylic acid) (pNIPAm-AAc) microgels and linear polycations as building blocks in 2003,[9] different groups have been conducting extensive research on the fabrication process and the thermal or pH responses and applications of these microgel films.[10−16] Although films composed of more than one type of microgel have been developed to modulate the film responsivity or swelling properties,[13,14] multilayer films composed entirely of microgel "bricks", without any linear or branched polyelectrolyte as the "mortar", have not yet been reported.

Previously, dried films on soft substrates were determined to undergo plastic deformation in response to linear strain, leading to film buckling upon strain relaxation. However, the buckling or wrinkling is readily healed by addition of water or even in the presence of high humidity environments,[17,18] with no apparent delamination and no evidence of remnant damage. Hydration leads to rapid reorganization of the film building blocks, permitting recovery of the film to the undamaged state.[18] However, preliminary results showed that films consisting of 1 μm carboxylated-modified polystyrene spheres and 400−500 K polydiallyldimethylammonium chloride[19] were not healed by hydration. Even for polymeric films assembled from branched poly(ethylenimine) and poly(acrylic acid), the healing capability largely depends on the structure and fabrication conditions.[20] Thus, the healing performance of films assembled from different building blocks requires further exploration to obtain a broader understanding of the parameters controlling self-healing.

In this letter, we synthesized self-cross-linked, anionic poly(*N*-isopropylacrylamide-*co*-acrylic acid) (pNIPAm-AAc) and cationic poly(*N*-isopropylacrylamide-*co*-(*N*-(3-aminopropyl) methacrylamide hydrochloride)) (pNIPAm-APMH) microgels in the absence of chemical cross-linkers by precipitation polymerization. All-microgel films were then fabricated by centrifugal deposition from a mixture of these two microgels without using any linear polyelectrolyte "mortar". Both isotropic and anisotropic stretching were applied to damage the dried film, and the formed damage patterns and film self-healing by hydration were studied.

Received: January 7, 2015
Accepted: February 17, 2015
Published: February 18, 2015

DOI: 10.1021/acsmacrolett.5b00016
ACS Macro Lett. 2015, 4, 302−307

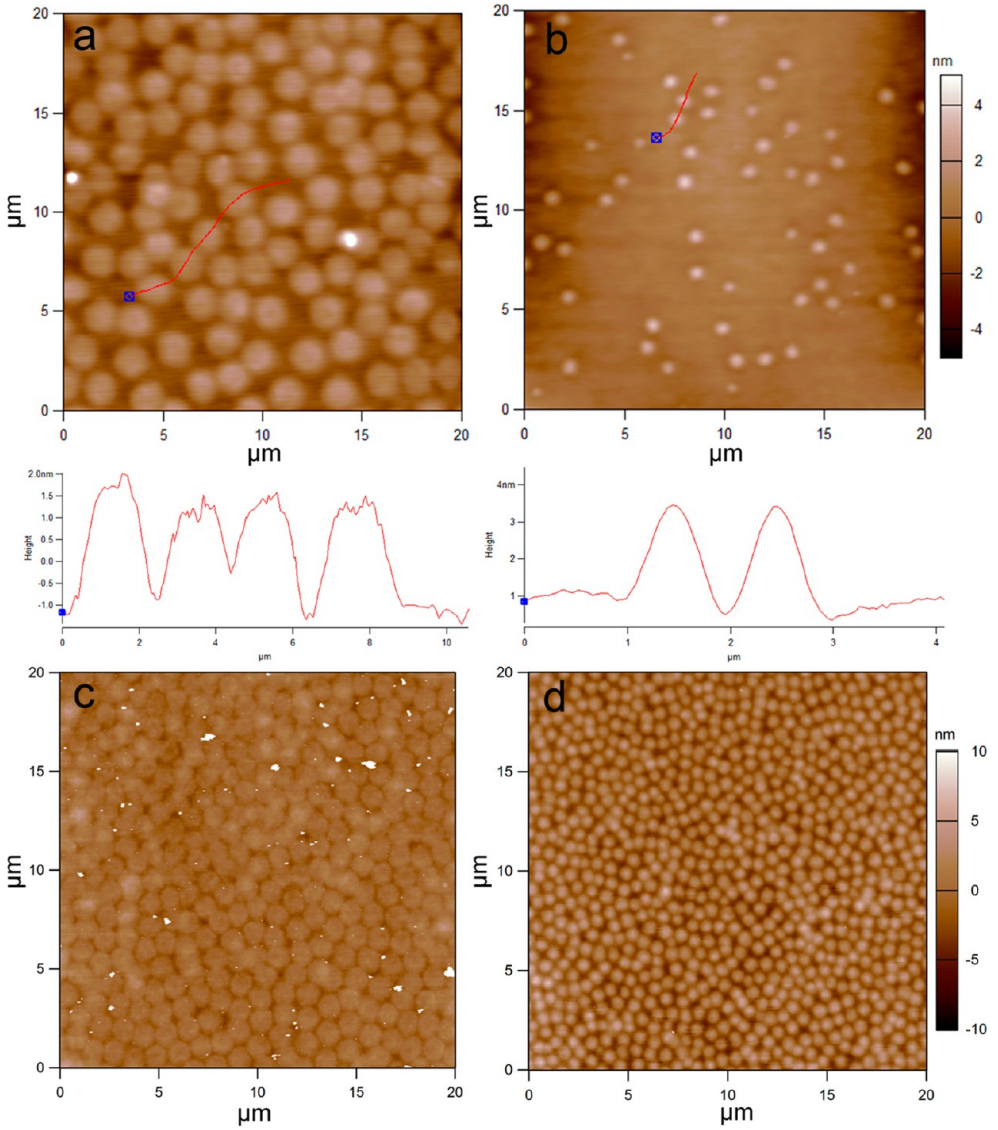

Figure 1. AFM height images and line profiles of absorbed (a) **A** ***μ*****gels** and (b) **C** ***μ*****gels** on glass substrates and their corresponding monolayer films (c) and (d) formed from centrifugal deposition. The *z*-scale for (a) and (b) is shown next to panel (b), and that for (c) and (d) is shown next to panel (d).

Self-cross-linked pNIPAm microgels were formed due to the chain transfer reaction during the polymerization.[21,23,24] Our most recent paper found that the self-cross-linked microgels were ultrasoft, displaying emergent platelet-like behaviors when modified with fibrinogen-binding motifs.[25] Self-cross-linked anionic pNIPAm-AAc microgels and cationic pNIPAm-APMH microgels were synthesized for film fabrication. Microgels alone were first characterized by DLS and AFM. DLS results show that the diameter of **A** ***μ*****gels** and **C** ***μ*****gels** in pH 6.5 buffer (100 mM ionic strength) are around 1.2 μm and 660 nm, respectively. In order to clearly visualize individual particles, an amine-functionalized glass coverslip was immersed into a dilute solution of **A** ***μ*****gels** for absorption. For the absorption of **C** ***μ*****gels**, the amine-functionalized coverslips were primed by first absorbing a layer of poly(sodium styrenesulfonate) on the surface. As illustrated in Figure 1, both microgels have a low degree of polydispersity. In both cases, severely flattened particles were formed due to the strong microgel−surface interactions, the softness of the microgels, and the fact that the particles are dehydrated. Line profiles taken from these images show that the diameters of the dried microgels are around 2.2 and 1 μm for **A** ***μ*****gels** and **C** ***μ*****gels**, respectively, while the heights are both less than 3 nm. This height is even lower than that of chemical cross-linked microgels with smaller hydrodynamic size,[22] illustrating the much lower polymer density and greater softness of the self-cross-linked microgels. Centrifugal deposition of microgels onto glass coverslips results in monolayer films with more closely packed microgels than those from chemical cross-linked microgel[22] (Figure 1c and d), which illustrates the good film-forming properties of self-cross-linked microgels.

For multilayer film fabrication using microgels and linear polyelectrolytes as building blocks, microgels and polyelectrolytes are alternatively deposited. In that method, before an additional microgel layer is added by centrifugal deposition, an oppositely charged polyelectrolyte layer must be formed by absorption. However, for the fabrication of all-microgel films, the process is potentially simpler since every layer can be added by centrifugal deposition. However, under certain conditions, we have found that two microgel layers (a bilayer) can be

DOI: 10.1021/acsmacrolett.5b00016
ACS Macro Lett. 2015, 4, 302−307

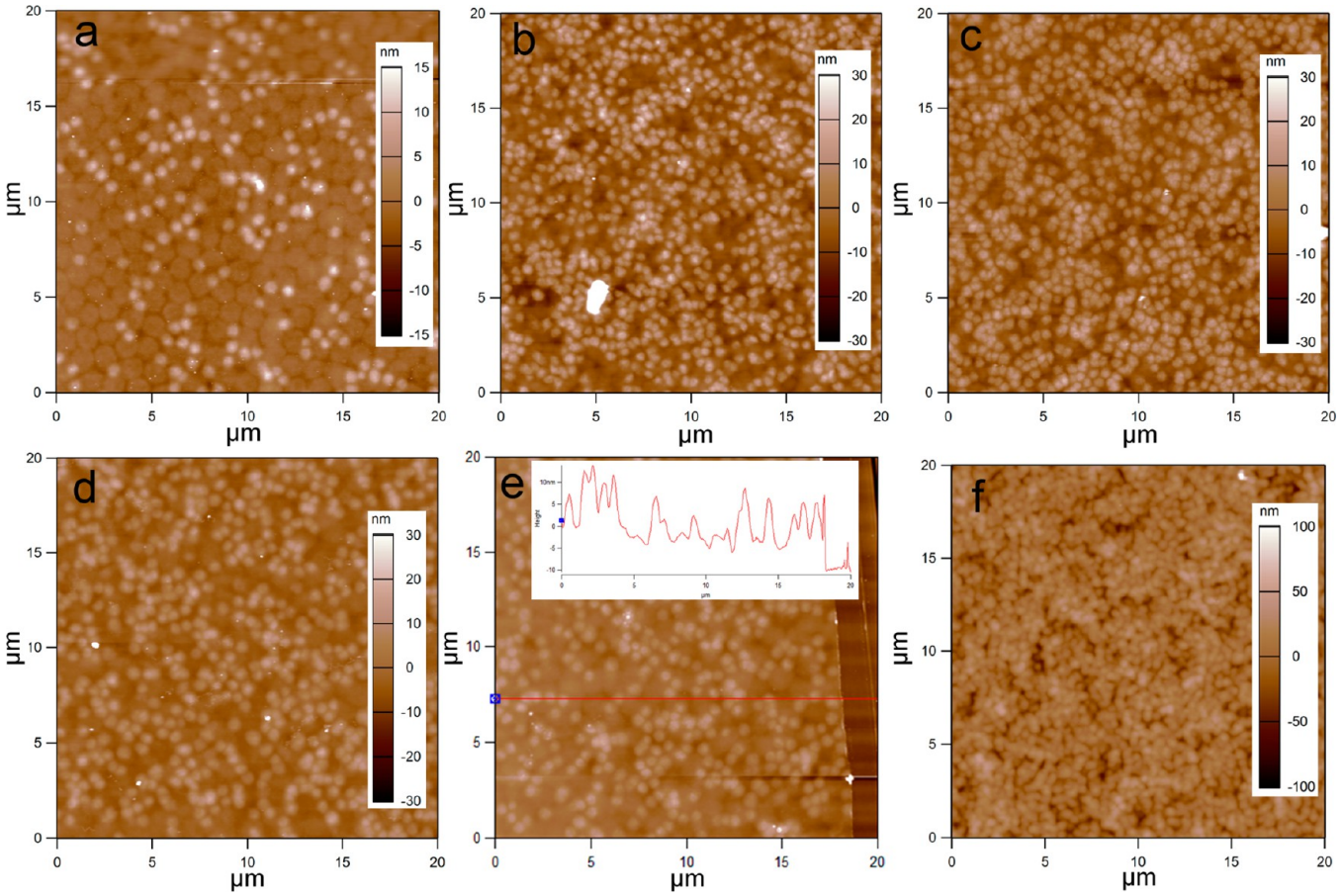

Figure 2. AFM height images of film from 10 min deposition from a mixture solution of 0.1 mg/mL **A *μ*gels** with (a) 0.01 mg/mL, (b) 0.05 mg/mL, or (c) 0.1 mg/mL **C *μ*gels**. AFM images of films from a solution of 0.1 mg/mL **A *μ*gels** and 0.1 mg/mL **C *μ*gels** with a different deposition time: (d) 5 min and (f) 30 min. (e) The thickness profile image of (d) microgel film.

deposited from a mixture of **A *μ*gels** and **C *μ*gels** during each centrifugation cycle. To optimize the required conditions, we studied the influence of the concentration of microgels and the centrifugal deposition time on the morphology of film. When fixing the centrifugation time of 10 min and 0.1 mg/mL of **A *μ*gels**, the increase of **C *μ*gels** concentration results in a higher packing density of **C *μ*gels** on the top layer (Figures 2a,b,c). When **C *μ*gels** concentration is as low as 0.01 mg/mL, the deposition results in a film with two obvious layers, a tightly packed layer of **A *μ*gels** on the bottom, and a loosely packed layer of **C *μ*gels** on the top (Figure 2a). With an increasing concentration of **C *μ*gels**, the packing density of the top layer increases, without obvious changes in the packing density of **A *μ*gels** in the first layer (Figures 2b and c). When the concentrations of **A *μ*gels** and **C *μ*gels** are both 0.1 mg/mL and the deposition time is reduced to 5 min (Figure 2d), the packing density of **C *μ*gels** on the top layer decreases, while a highly packed bottom layer of **A *μ*gels** is still achieved. These results suggest that the larger **A *μ*gels** appear to reach full coverage faster than the smaller **C *μ*gels**. This is expected because of larger or more massive particles having a higher sedimentation velocity. The profile image in Figure 2e clearly shows the two-layer character of the film and the thickness of this bilayer film, with each layer being around 10 nm. However, 30 min centrifugation deposition results in a thick film (250 nm) (Figure 2f). With these long centrifugation times, most **A *μ*gels** and **C *μ*gels** were deposited to the surface. During repeated washing with DI water, we propose that there is a particle rearrangement on the substrate surface. Part of the microgels with only repulsive neighboring microgels will be washed away, while microgels together with attractive neighboring microgels likely stay on the surface to form a stable film. Thus, the deposition is not self-limiting, and thick films can be formed using longer deposition times, if desired.

As discussed before, a 10 min centrifugal deposition from a mixture containing 0.1 mg/mL **A *μ*gels** and 0.1 mg/mL **C *μ*gels** results in a bilayer film. We use this condition to fabricate multilayer films by LbL assembly as shown in Figure 3a, wherein the bilayer films are rinsed and dried between each centrifugal deposition. The microgel films here are denoted as AC(n), where n indicates the number of bilayers. From the height image of the AC(5) film (Figure 3b), it is hard to distinguish between the **A *μ*gels** and **C *μ*gels** as they both appear smaller than those shown in Figure 1c and d. This likely arises from microgel deswelling due to an increase in the local osmotic pressure during the microgel film assembly.[26,27]

The thickness of the film was monitored after every centrifugal deposition by AFM line profiles across a scratch in the film introduced by a clean razor blade. Figure 4a confirms that one centrifugal deposition results in a bilayer film, with a thickness of around 20 nm. The thickness increases linearly with number of bilayers (number of deposition times) with an increase of ~25 nm/bilayer. After nine depositions, the thickness reaches ~200 nm.

To interrogate how controlled stretching of the film impacts film structure, two different stretching methods were used to

DOI: 10.1021/acsmacrolett.5b00016
ACS Macro Lett. 2015, 4, 302−307

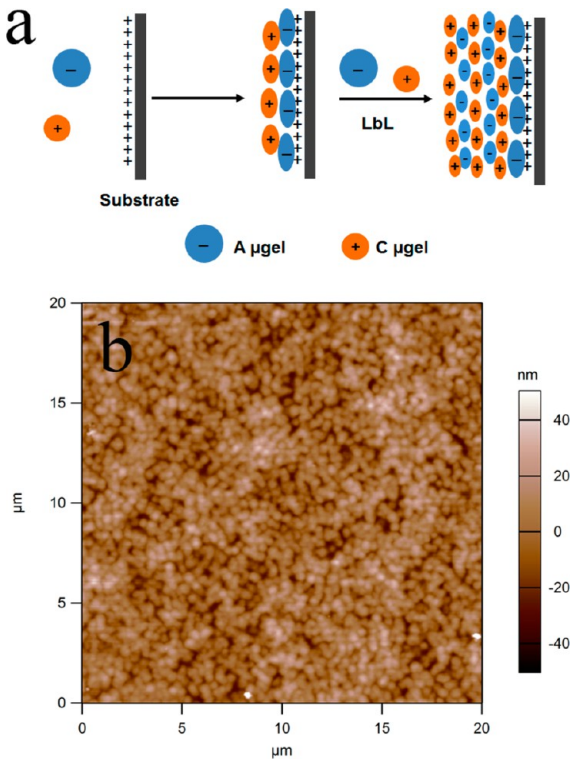

Figure 3. (a) Microgel films by centrifugation deposition from a mixture solution of **A *μ*gels** and **C *μ*gels**. (b) AFM height image of AC(5) film.

damage the dried films on PDMS. As shown in Figure 5b, 20% uniaxial strain causes almost parallel wrinkles in the film that are perpendicular to the stretching direction, which is in accord with the results obtained with microgel–polyelectrolyte films.[18] Upon stretching, the total area of the film increases to accommodate the stretching of the elastomeric substrate. Removing the stress reduces the effective area of the substrate, while the film lacks the elasticity needed to return to its original area, thus resulting in wrinkling. However, the damaged film can be easily healed after addition of water due to the swelling and rearrangement of microgels (Figure 5c). Another way to deform the film is through thermal treatment of the PDMS underlying the microgel films. Thermal expansion and subsequent cooling of the film creates compressive stress in the film that is relieved by buckling. Because the PDMS expands and contracts isotropically, the resulting buckling patterns are no longer oriented in one direction (Figures 5d and f), creating patterns that are similar to those observed from the buckling of metal films deposited on PDMS.[28] With an increase of thermal treatment temperature, the buckling density increases. Different from the thermal treatment at 100 °C, thermal treatment at 150 °C induces the cross-linking between carboxylate groups of **A *μ*gels** and amine groups of **C *μ*gels** by formation of amides,[29−31] significantly increasing the stiffness of the microgel film, which then requires a greater degree of buckling to release the compressive stress. After the addition of water, damage caused by 100 °C treatment is healed (Figure 5e), but damage induced by the 150 °C treatment cannot be healed (Figure 5f). The cross-linking between microgels largely limits the mobility of building blocks, which results in poor healing characteristics.[32] It is important to point out that these wrinkling defects do not occur on silanized PDMS alone and are exclusively associated with the microgel films.

In this investigation it has been shown that all-microgel thin films from anionic and cationic self-cross-linked microgels can be assembled by a LbL approach. Importantly, we find that one centrifugal deposition from a mixture of the two microgels can produce a bilayer film, which therefore provides a more efficient way to fabricate all-microgel films. We have also found that thermal expansion of PDMS is an effective way to generate microgel film wrinkling, where the pattern itself and the self-healing properties are dependent upon the treatment temperature. We hypothesize that the surface wrinkling pattern is adjustable by changing the film thickness and PDMS shape,

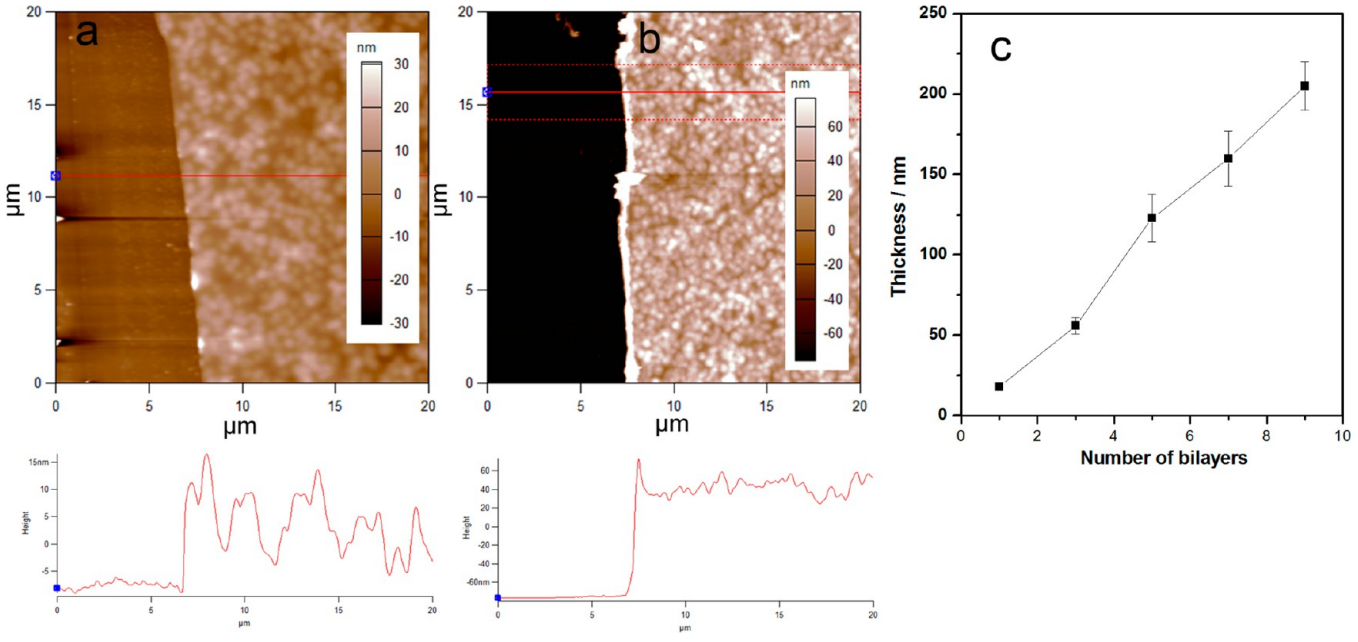

Figure 4. AFM images of (a) AC(1) and (b) AC(5) microgel films and (c) the thickness of films with different number of bilayers. Error bars in (c) are the standard deviation of five spot measurements on a single film.

DOI: 10.1021/acsmacrolett.5b00016
ACS Macro Lett. 2015, 4, 302−307

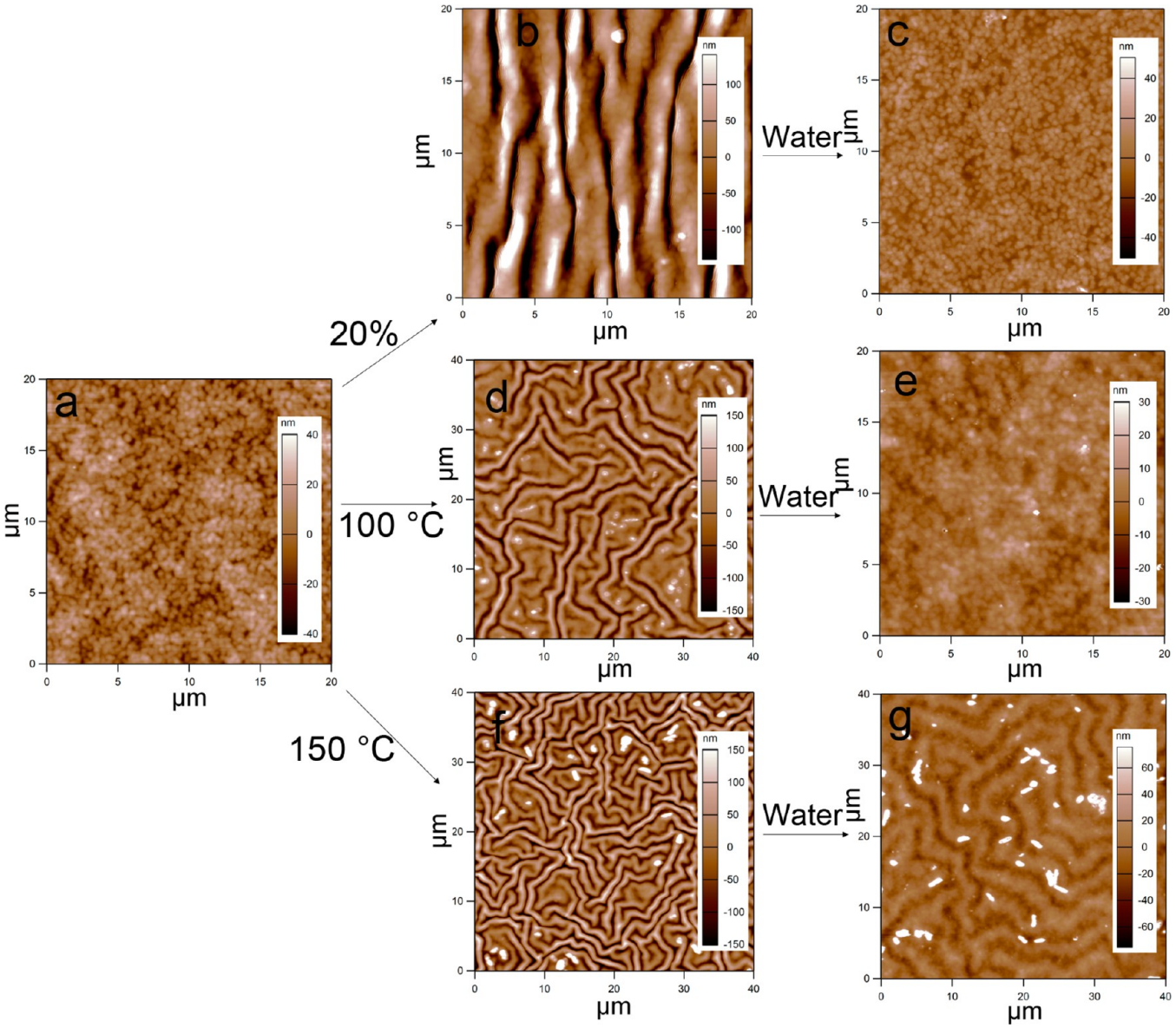

Figure 5. AFM images of (a) undamaged AC(5) microgel film on PDMS, (b) after 20% anisotropic stretching, or after thermal treatment at (d) 100 °C and (f) 150 °C. The corresponding images after the addition of water are shown in (c, e, g).

which requires a more detailed study. This kind of surface wrinkling of films can also offer a simple yet elegant approach to fabricating cell culture substrate with desired topographies for investigating cell mechanobiology.[33−35]

EXPERIMENTAL SECTION

Materials. All materials were purchased from Sigma-Aldrich unless otherwise noted. NIPAm was purified by recrystallization from *n*-hexane (VWR International). Reagents AAc, APMH, and ammonium persulfate (APS) were used as received. Water was produced by distillation followed by deionization to a resistance of 18 MΩ cm (Barnstead E-Pure system), followed by filtration through a 0.2 μm filter to remove particulate matter.

Microgel Synthesis and Characterization. For both microgel syntheses, the total monomer concentration was 140 mM, with a molar composition of 90% NIPAm and 20% AAc for anionic microgels and 95% NIPAm and 5% APMH for cationic microgels. No chemical cross-linkers were added. The procedure is the same as standard precipitation polymerization at 70 °C using 2 mM APS solution, as previously described.[21] Here, pNIPAm-AAc microgels are denoted **A *μ*gels**, while pNIPAm-APMH microgels are denoted **C *μ*gels**. Dynamic light scattering (DLS, Protein Solutions DynaPro DLS) was used to measure the hydrodynamic radius of synthesized particles in phosphate buffer (pH 6.5, 100 mM ionic strength).

Microgel Film Deposition. Two substrate types, glass coverslips (22 mm × 22 mm) and poly(dimethylsiloxane) (PDMS) sheets, were prepared and functionalized according to our previous work and then used for film deposition.[17] Cleaned and dried glass coverslips or PDMS were individually placed at the bottom of six-well plates, which were then filled with a PBS buffer (pH 6.5, 100 mM ionic strength) solution of a mixture of **A** and **C *μ*gels**. A maximum total microgel concentration of 0.2 mg/mL and buffer with relatively high ionic strength of 100 mM was used here to avoid flocculation. The well plates were placed immediately across from a counter-weighted well plate in an Eppendorf 5804R centrifuge equipped with a plate-holding rotor.[22] Films were centrifugally deposited at a relative centrifugal force (rcf) of 2250*g* for a designed time. Films were then gently rinsed with deionized water and dried under a gentle stream of N_2. Additional layers were then repeatedly deposited as described above until the desired layer number was achieved.

DOI: 10.1021/acsmacrolett.5b00016
ACS Macro Lett. 2015, 4, 302−307

Film Stretching and Healing. Films were stretched in an anisotropic or isotropic way. The anisotropic stretching was achieved by using a homemade stretching apparatus that was capable of precisely controlling the degree of applied strain.[14] Samples, with the coated side up, were carefully fixed to a micrometer-controlled, single-axis translation stage. Then a stress was applied to stretch the PDMS to a strain of 20%. Isotropic stretching was achieved by PDMS thermal expansion. PDMS, which had been coated with microgel film, was put in a 100 or 150 °C oven for 2 h and then allowed to cool to room temperature. To allow the PDMS to expand or contract isotropically, we separated the PDMS from the glass slide with a paper tissue. In order to check the healing capability of damaged films, the stretched films were put into deionized water for 5 min and then dried under a gentle stream of N_2.

Film Characterization. Films were imaged using an Asylum Research MFP-3D AFM (Santa Barbara, CA). Noncontact mode aluminum-coated silicon nitride cantilevers were purchased from NanoWorld (force constant = 42 N/m, resonance frequency = 320 kHz). All images were taken in air under ambient conditions. Film thickness was measured using a method previously described by our group.[18] The region of the scratch was imaged, and then the images were analyzed by averaging the results from 3 μm wide traces wherein the surfaces of the film and the glass substrate were clearly discernible. The height difference between the substrate and the film was used to determine the thickness.

AUTHOR INFORMATION

Corresponding Author

*E-mail: lyon@chapman.edu.

Notes

The authors declare no competing financial interest.

ACKNOWLEDGMENTS

This work was supported by the Georgia Institute of Technology.

REFERENCES

(1) Decher, G. *Science* **1997**, *277*, 1232−1237.
(2) Zhang, X.; Chen, H.; Zhang, H. Y. *Chem. Commun.* **2007**, 1395−1405.
(3) Such, G. K.; Johnston, A. P. R.; Caruso, F. *Chem. Soc. Rev.* **2011**, *40*, 19−29.
(4) Lee, D.; Rubner, M. F.; Cohen, R. E. *Nano Lett.* **2006**, *6*, 2305−2312.
(5) Lyon, L. A.; Meng, Z. Y.; Singh, N.; Sorrell, C. D.; John, A. S. *Chem. Soc. Rev.* **2009**, *38*, 865−874.
(6) Salomaki, M.; Vinokurov, I. A.; Kankare, J. *Langmuir* **2005**, *21*, 11232−11240.
(7) Wong, J. E.; Richtering, W. *Curr. Opin Colloid Interface Sci.* **2008**, *13*, 403−412.
(8) Wong, J. E.; Diez-Pascual, A. M.; Richtering, W. *Macromolecules* **2009**, *42*, 1229−1238.
(9) Serpe, M. J.; Jones, C. D.; Lyon, L. A. *Langmuir* **2003**, *19*, 8759−8764.
(10) Nolan, C. M.; Serpe, M. J.; Lyon, L. A. *Biomacromolecules* **2004**, *5*, 1940−1946.
(11) Serpe, M. J.; Lyon, L. A. *Chem. Mater.* **2004**, *16*, 4373−4380.
(12) Serpe, M. J.; Yarmey, K. A.; Nolan, C. M.; Lyon, L. A. *Biomacromolecules* **2005**, *6*, 408−413.
(13) Clarke, K. C.; Lyon, L. A. *Langmuir* **2013**, *29*, 12852−12857.
(14) Zhang, L.; Spears, M. W.; Lyon, L. A. *Langmuir* **2014**, *30*, 7628−7634.
(15) Hofl, S.; Zitzler, L.; Hellweg, T.; Herminghaus, S.; Mugele, F. *Polymer* **2007**, *48*, 245−254.
(16) Schmidt, S.; Motschmann, H.; Hellweg, T.; von Klitzing, R. *Polymer* **2008**, *49*, 749−756.
(17) South, A. B.; Lyon, L. A. *Angew. Chem., Int. Ed.* **2010**, *49*, 767−771.
(18) Gaulding, J. C.; Spears, M. W.; Lyon, L. A. *Polym. Chem.* **2013**, *4*, 4890−4896.
(19) South, A. B., Assembly and Dynamic Behavior of Microgel Thin Films and Their Application to Biointerfaces. Georgia Institute of Technology, 2010.
(20) Wang, X.; Liu, F.; Zheng, X. W.; Sun, J. Q. *Angew. Chem., Int. Ed.* **2011**, *50*, 11378−11381.
(21) Hu, X. B.; Tong, Z.; Lyon, L. A. *Langmuir* **2011**, *27*, 4142−4148.
(22) South, A. B.; Whitmire, R. E.; Garcia, A. J.; Lyon, L. A. *ACS Appl. Mater. Interfaces* **2009**, *1*, 2747−2754.
(23) Gao, J.; Frisken, B. J. *Langmuir* **2003**, *19*, 5217−5222.
(24) Gao, J.; Frisken, B. J. *Langmuir* **2005**, *21*, 545−551.
(25) Brown, A. C.; Stabenfeldt, S. E.; Ahn, B.; Hannan, R. T.; Dhada, K. S.; Herman, E. S.; Stefanelli, V.; Guzzetta, N.; Alexeev, A.; Lam, W. A.; Lyon, L. A.; Barker, T. H. *Nat. Mater.* **2014**, *13*, 1108−1114.
(26) St John, A. N.; Breedveld, V.; Lyon, L. A. *J. Phys. Chem. B* **2007**, *111*, 7796−7801.
(27) St John, A. N.; Lyon, L. A. *J. Phys. Chem. B* **2008**, *112*, 11258−11263.
(28) Bowden, N.; Brittain, S.; Evans, A. G.; Hutchinson, J. W.; Whitesides, G. M. *Nature* **1998**, *393*, 146−149.
(29) Harris, J. J.; DeRose, P. M.; Bruening, M. L. *J. Am. Chem. Soc.* **1999**, *121*, 1978−1979.
(30) Mallwitz, F.; Laschewsky, A. *Adv. Mater.* **2005**, *17*, 1296−+.
(31) Shao, L.; Lutkenhaus, J. L. *Soft Matter* **2010**, *6*, 3363−3369.
(32) Saxena, S.; Spears, M. W.; Yoshida, H.; Gaulding, J. C.; Garcia, A. J.; Lyon, L. A. *Soft Matter* **2014**, *10*, 1356−1364.
(33) Yang, P.; Baker, R. M.; Henderson, J. H.; Mather, P. T. *Soft Matter* **2013**, *9*, 4705−4714.
(34) Yim, E. K. F.; Reano, R. M.; Pang, S. W.; Yee, A. F.; Chen, C. S.; Leong, K. W. *Biomaterials* **2005**, *26*, 5405−5413.
(35) Khetan, S.; Burdick, J. A. *Soft Matter* **2011**, *7*, 830−838.

DOI: 10.1021/acsmacrolett.5b00016
ACS Macro Lett. 2015, 4, 302−307